

A B-Spline Higher Order Panel Method Applied to the Radiation Wave Problem for a 2-D Body Oscillating on the Free Surface

D.-C. Hong¹, C.-S. Lee²

¹ Researcher, Center for Advanced Transportation Vehicles, Chungnam National University, Taejon, Korea

² Professor, Department of Naval Architecture & Ocean Engineering, Chungnam National University, Taejon, Korea

Abstract

The improved Green integral equation using the Kelvin-type Green function is known free of irregular frequencies where the integral over the inner free surface ensures the square-integrable property of the kernel. In this paper, the inner free surface integral is removed from the integral equation, resulting in an overdetermined integral equation. The solution of the overdetermined Green integral equation is shown identical with the solution of the improved Green integral equation. Using the B-spline higher order panel method, the overdetermined equation is discretized in two different ways; one of the resulting linear system is square and the other is redundant. Numerical experiments show that the solutions of both are identical. Using the present methods, the exact values and higher derivatives of the potential at any place over the wetted surface of the body can be found with much fewer panels than low order panel methods.

Keywords : Kelvin-type Green function, Overdetermined Green integral equation, B-splines, Higher order panel method, Radiation wave

1 Introduction

Discretization of an integral equation and solving the resulting linear system are known as the panel method which has been developed in the fields of hydrodynamics and aerodynamics since the pioneering work of Hess and Smith[Hess & Smith, 1964]. The present paper deals with the numerical solution of the improved Green integral equation[Hong, 1984] which is free of the irregular frequencies. The irregular frequencies are present in the solution of the Kelvin-type Green integral equation in the frequency domain for the radiation wave problem of the oscillating surface-piercing body[Guevel & Kobus, 1975]. The existence and uniqueness of the solution of the improved Green integral equation has been shown by Hong[Hong, 1987] where the integral over the inner free surface ensures the coincidence of the domain of integration with the range of the integral equation. The discretization according to the low order panel method yields a square linear system which can easily be solved by the usual Gauss elimination. There are other

methods which can eliminate certain of the irregular frequencies in the least square sense. One of them, due to Kobus[Kobus, 1976], allows the linearity on the first and last panels adjacent to the free surface, introducing two additional unknowns(the potential variation within the panel) to the original low order panel method. To yield a square linear system, he then added the null potential condition to the two extra control points on the inner free surface. This method is simpler than the improved Green integral equation due to the absence of inner free surface integral, but cannot eliminate all irregular frequencies and is vulnerable to numerical instability originating from the junction of the linear and constant panels. The other, due to Ohmatsu[Ohmatsu, 1983], is to apply two additional(null potential and zero horizontal velocity) conditions at a control point on the inner free surface. The resulting linear system, being overdetermined, is solved by a least square approach.

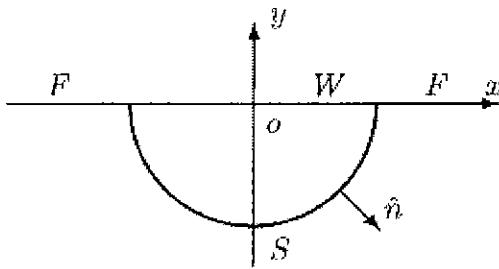


Figure 1. Coordinate System.

In this paper, the kernel of the improved Green integral equation will be reduced so that the inner free surface integral may disappear. Thus the range of the integral equation is larger than the domain of integration. Discretizing this, say, overdetermined¹ Green integral equation according to the low order panel method yields an overdetermined linear system. It will be shown that the solution of this system is identical with that of the former square system. Finally, by making use of the B-spline higher order panel method, the overdetermined

Green integral equation will be discretized in two different ways. One of the resulting linear system is square and the other is redundant². The former is a square system even though the integral equation is overdetermined and can easily be solved by the usual Gauss elimination.

2 Overdetermined Green Integral Equation

The fluid is assumed to occupy a space bounded by the wetted surface S of a surface-piercing cylindrical body and by the free surface F of deep water under gravity. Cartesian coordinates $\vec{x} = (x, y)$ attached to the mean position of the body, are employed with the origin o in the waterplane W of the cylindrical body of which the generators are perpendicular to the complex plane $z = x + iy$, the x axis coinciding with the undisturbed free surface, the y axis vertically upward as shown in Figure 1. The body performs simple harmonic oscillations of small amplitude about its mean position with circular frequency ω . With the usual assumption of an incompressible fluid and an irrotational flow, the fluid velocity is given by the gradient of a velocity potential $\varphi = Re\{\Phi e^{-i\omega t}\}$ where Φ denotes the complex valued radiation potential.

The first-order motion of the body can be described as follows:

$$\vec{A} = Re\{(a_1\hat{e}_1 + a_2\hat{e}_2 + a_3\hat{e}_3 \times \vec{OQ})e^{-i\omega t}\} \quad (1)$$

¹the terminology "overdetermined" is used in a sense that the range of the integral equation is greater than the domain of integration.

²the terminology "redundant" is used in a sense that the number of control points is selected more than needed.

where \vec{A} is displacement vector of a point Q on S , O the roll center, and $a_j (j = 1, 2, 3)$ denote respectively the complex amplitude of sway, heave and roll. The potential Φ is usually expressed as follows:

$$\Phi = -i\omega \sum_{m=1}^3 a_m \phi_m \quad (2)$$

where ϕ_m is the complex valued elementary potential associated with the unit amplitude motion of mode m . The governing equation, the first-order free surface and body boundary conditions for $\phi_m (m = 1, 2, 3)$ are as follows:

$$\nabla^2 \phi_m = 0 \quad \text{in fluid region, } m = 1, 2, 3 \quad (3)$$

$$-k_o \phi_m + \frac{\partial \phi_m}{\partial y} = 0 \quad \text{on } y = 0, \quad m = 1, 2, 3 \quad (4)$$

$$\frac{\partial \phi_m}{\partial n} = \hat{e}_m \cdot \hat{n} \quad \text{on } S, \quad m = 1, 2 \quad (5)$$

$$\frac{\partial \phi_3}{\partial n} = (\hat{e}_3 \times \vec{OQ}) \cdot \hat{n} \quad \text{on } S \quad (6)$$

where \hat{n} denotes a normal vector directed into the fluid region from S and $k_o = \omega^2/g$ the wavenumber. The potential must also satisfy the radiation condition at infinity.

By making use of Kelvin-type Green function which satisfies the free surface boundary condition as well as the radiation condition at infinity, the value of $\phi_m (m = 1, 2, 3)$ at a point P in fluid region can be found as follows:

$$\phi_m(P) = \int_S \left[\frac{\partial \phi_m(Q)}{\partial n_Q} G(P, Q) - \phi_m(Q) \frac{\partial G(P, Q)}{\partial n_Q} \right] ds_Q \quad (7)$$

where G is the Kelvin-type Green function represented in the complex plane $z = x + iy$ as follows:

$$G(P, Q) = G_o + G_i + G_f \quad (8)$$

with

$$G_o(P, Q) = \frac{1}{2\pi} \text{Re} \{ \log(z_P - z_Q) \} \quad (9)$$

$$G_i(P, Q) = -\frac{1}{2\pi} \text{Re} \{ \log(z_P - \bar{z}_Q) \} \quad (10)$$

$$G_f(P, Q) = -\frac{1}{2\pi} \text{Re} \{ (2J[-ik_o(z_P - \bar{z}_Q)]) \} - i \text{Re} \left\{ e^{-ik_o(z_P - \bar{z}_Q)} \right\} \quad (11)$$

where

$$J(\zeta) = e^\zeta [\mathcal{E}_1(\zeta) + i\pi] \quad (12)$$

and \mathcal{E}_1 is the modified complex exponential integral[Guevel & Kobus, 1975].

The normal derivatives of potential on S , $\partial \phi_m(Q)/\partial n_Q$, known by the body boundary conditions (5) and (6), and the value of potential on $S \cup W$, $\phi_m(Q)$, can be found as the solution of the improved Green integral equation:

$$\mathcal{A}(P)\phi_m(P) + \int_{S \cup W} \phi_m(Q) \frac{\partial G'(P, Q)}{\partial n_Q} ds_Q = \int_S \frac{\partial \phi_m(Q)}{\partial n_Q} G'(P, Q) ds_Q, \quad P \text{ on } S \cup W \quad (13)$$

where G' is the modified Kelvin-type Green function as follows

$$G'(P, Q) = G_o + G_i + G_f[1 - \delta(y_P - 0)\delta(y_Q - 0)] \quad (14)$$

and

$$\mathcal{A}(P) = \begin{cases} 1/2 & \text{for } Q \in S \text{ and } P = Q \\ 1 & \text{for } Q \in W \text{ and } P = Q \\ 0 & \text{otherwise} \end{cases} \quad (15)$$

Discretizing (13) according to the low order panel method, one can find an M by M linear system(denoted **imGrLo** in Tables and Figures)

$$\begin{bmatrix} \mathbf{A}_{11} & \mathbf{A}_{12} \\ \mathbf{A}_{21} & \mathbf{I} \end{bmatrix} \begin{Bmatrix} \phi_1 \\ \vdots \\ \phi_M \end{Bmatrix} = \begin{Bmatrix} B_1 \\ \vdots \\ B_M \end{Bmatrix} \quad (16)$$

where the elements of submatrices are defined as follows.

For $i = 1, \dots, N$,

$$\{\mathbf{A}_{11}\}_{i,j} = \int_{\Delta s_j} \frac{\partial G(P_i, Q)}{\partial n_Q} ds_Q, \quad \text{for } j = 1, \dots, N \quad (17)$$

For $i = 1, \dots, N$,

$$\{\mathbf{A}_{12}\}_{i,j} = \int_{\Delta s_{N+j}} \frac{\partial G(P_i, Q)}{\partial n_Q} ds_Q, \quad \text{for } j = 1, \dots, M - N \quad (18)$$

For $i = 1, \dots, M - N$,

$$\{\mathbf{A}_{21}\}_{i,j} = \int_{\Delta s_j} \frac{\partial G(P_{N+i}, Q)}{\partial n_Q} ds_Q, \quad \text{for } j = 1, \dots, N \quad (19)$$

and the elements of the right-hand side vector are, for $i = 1, \dots, M$,

$$B_i = \sum_{j=1}^N \frac{\partial \phi(Q_j)}{\partial n_{Q_j}} \int_{\Delta s_j} G(P_i, Q) ds_Q \quad (20)$$

where N is the number of panels on S and $M - N$ the number of panels on W . Note that the submatrix \mathbf{I} is an identity matrix, since G_f in (14) vanishes when P and Q lie simultaneously on W .

From the theory of integral equation, the solution of (16) by the usual Gauss elimination converges to the solution of (13) as the number M tends to infinity. A modified Green integral

equation similar to the equation (13) has been developed by Kleinman[Kleinman, 1982]. However, since the original Kelvine-type Green function (8) was employed in his modified integral equation, its solution is different from that of the improved Green integral equation employing the modified Kelvine-type Green function as shown in (14).

If this linear system is reduced so that the submatrices \mathbf{A}_{12} , \mathbf{A}_{21} and \mathbf{I} disappear, an N by N linear system(denoted **GrLo** in Tables and Figures) can be found.

$$\begin{bmatrix} \mathbf{A}_{11} \end{bmatrix} \begin{Bmatrix} \phi_1 \\ \vdots \\ \phi_N \end{Bmatrix} = \begin{Bmatrix} B_1 \\ \vdots \\ B_N \end{Bmatrix} \quad (21)$$

This linear system can also be found from the original Green integral equation with the Kelvin-type Green function as follows[John, 1950]:

$$\mathcal{A}(P)\phi_m(P) + \int_S \phi_m(Q) \frac{\partial G(P, Q)}{\partial n_Q} ds_Q = \int_S \frac{\partial \phi_m(Q)}{\partial n_Q} G(P, Q) ds_Q, \quad P \text{ on } S \quad (22)$$

where

$$\mathcal{A}(P) = \begin{cases} 1/2 & \text{for } P = Q \\ 0 & \text{otherwise} \end{cases} \quad (23)$$

It is well known that the solution of (22) is undetermined when k_o coincides to the one of its irregular frequencies.

Now, if the the submatrices \mathbf{A}_{12} and \mathbf{I} are removed from the linear system (16), an overdetermined M by $N(M > N)$ linear system(denoted **ovGrLo** in Tables and Figures) can be obtained as

$$\begin{bmatrix} \mathbf{A}_{11} \\ \mathbf{A}_{21} \end{bmatrix} \begin{Bmatrix} \phi_1 \\ \vdots \\ \phi_N \end{Bmatrix} = \begin{Bmatrix} B_1 \\ \vdots \\ B_M \end{Bmatrix} \quad (24)$$

The reduced matrix has independent columns since the columns of the full square matrix in the system, **imGrLo**, (16) are independent. It follows that the system, **ovGrLo**, (24) has at most one solution for every \mathbf{B} which is common for the two systems. If the forcing vector \mathbf{B} also lies in the column space of the reduced matrix, the system (24) will have one solution identical with the solution of (16). However, it is also possible that \mathbf{B} does not lie in the reduced column space. In this case, the solution of (24) is identical with the solution of (16) provided that ϕ vanishes on the inner free surface W . Since the system (24) comprises the necessary condition for the vanishment of ϕ on W , \mathbf{B} should always lie in the reduced column space, and hence the solution of the system (24) is identical with the solution of (16). From the integral equation point of view, the system (24) is a discretized form of the overdetermined Green integral equation as follows:

$$\mathcal{A}(P)\phi_m(P) + \int_S \phi_m(Q) \frac{\partial G(P, Q)}{\partial n_Q} ds_Q = \int_S \frac{\partial \phi_m(Q)}{\partial n_Q} G(P, Q) ds_Q, \quad P \text{ on } S \cup W \quad (25)$$

where

$$\mathcal{A}(P) = \begin{cases} 1/2 & \text{for } Q \in S \text{ and } P = Q \\ 0 & \text{otherwise} \end{cases} \quad (26)$$

3 B-spline Geometry and Potential Representation

Following Lee and Kerwin[Lee & Kerwin, 1999], we will adopt the p -th degree B-spline basis functions to represent the curves and then express the curves as a weighted sum of basis functions as

$$\vec{x}(u) = \sum_{j=0}^{\tilde{N}^v-1} \vec{x}_j^v \tilde{N}_j(u) \quad (27)$$

where u is the parameter, monotonically increasing along a curve, $\tilde{N}_j(u)$ the p -th degree B-spline basis functions, \vec{x}_j^v the geometric control vertices, \tilde{N}^v the number of geometric control vertices. $\tilde{N}_j(u)$ are in general rational functions of the parameter u , but in this paper we will consider only the non-rational (integral) B-splines. The approach developed here can be directly applied to geometry represented by NURBS without any difficulty.

Our ultimate goal is to solve for the velocity potential $\phi(s)$ along the surface of the body. However, instead of treating the potential directly, we will represent the potential as a weighted sum of B-spline basis functions in a similar form as for the geometry as

$$\phi(u) = \sum_{j=0}^{N^v-1} \phi_j^v N_j(u) \quad (28)$$

where $N_j(u)$ are the B-spline basis functions, ϕ_j^v the potential control vertices and N^v the number of potential control vertices. The number of potential control vertices N^v and the basis function $N_j(u)$ may be different from the corresponding quantities for the geometry, but the usable parametric space of the geometry and the potential should be identical. With the introduction of the potential vertices, the unknowns of the hydrodynamic problem are now the values of the potential vertices, ϕ_j^v , which are not the potential in the physical sense.

4 Discretization of Integral Equation

Discretization of the body surface in (25) into a set of N^ϕ panels will then yield

$$\frac{\phi}{2} + \sum_{n=0}^{N^\phi-1} \int_n \phi \frac{\partial G}{\partial n} ds = \sum_{n=0}^{N^\phi-1} \int_n \frac{\partial \phi}{\partial n} G ds \quad (29)$$

If the equation (28) is inserted into (29), we obtain for the control point on the i -th panel the following

$$\frac{1}{2} \sum_j N_j(u) \phi_j^v + \sum_n \sum_j \phi_j^v \int_n N_j(u) \frac{\partial G}{\partial n} ds = \sum_n \int_n \frac{\partial \phi}{\partial n} G ds \quad (30)$$

It should be noticed that the n summation for the dipole over the panels in (30) includes the case of self-induction, that is the case when the control point falls within the panel boundary. In the low order panel method, this term drops out, since the effect is already considered by the subtended angle of the circle surrounding the point where the potential is evaluated. In the higher-order panel method, there are additional effects from the curvature or higher order variation of the geometry and the higher order variation of the potential in addition to the subtended angle effect.

5 Desingularization of Induction Integrals

When the control point falls within the singularity panel boundary, the function G_o in (8), known as the Rankine-type Green function, contains a logarithmically singular point, for which a special treatment is required for evaluation of the induction integral. The other two functions G_i and G_f in (8) are regular over the range of the overdetermined Green integral equation.

The singular behavior is most prominent when the coefficient of B-spline basis functions is constant in (30). Lee and Kerwin[Lee & Kerwin, 1999] showed that the singularity can be removed from the integral, and part of their work will be repeated here for completeness.

5.1 Self-Induced Potential of Rankine Sources

The induction integral of the Rankine source can also be split into two segments at the control point as follows:

$$\begin{aligned} I_{0,self}^S &= \left(\int_0^{s_R^*} + \int_0^{s_L^*} \right) \frac{\partial \phi}{\partial n} \frac{1}{2\pi} \log r ds^* \\ &\equiv I_{0,self,L}^S + I_{0,self,R}^S \end{aligned} \quad (31)$$

where the curvilinear coordinate s^* increases from the origin located at the control point to both sides of the panel and $r = |\vec{x}_P - \vec{x}_Q|$. The strength of the source is known from the oncoming flow, and can be expressed in power series of local curvilinear coordinate s^* as:

$$\left(\frac{\partial \phi}{\partial n} \right)_j \simeq \sum_{b=0}^p \alpha_{j,b}^* s^{*b} \quad (32)$$

Note that the local girthlength s^* is introduced to remove the singularity in (31), as will be shown in the following paragraphs.

The potential induced by the source at the control point located at one edge of the source panel can be computed by introducing the series expansion for the source strength (32) as

$$\begin{aligned} I_{0,self,R}^S &= \int_0^{s_R^*} \frac{\partial \phi}{\partial n} \frac{1}{2\pi} \log r ds^* \\ &\simeq \sum_b \alpha_{j,b}^* \int_0^{s_R^*} s^{*b} \frac{1}{2\pi} \log r ds^* \\ &= \sum_b \alpha_{j,b}^* \int_0^{s_R^*} s^{*b} \frac{1}{2\pi} \{ \log s^* + \log(r/s^*) \} ds^* \\ &= \sum_b \alpha_{j,b}^* \left\{ \frac{1}{2\pi} \left[\frac{s^{*b+1}}{b+1} \log s^* - \frac{s^{*b+1}}{(b+1)^2} \right]_0^{s_R^*} + \int_0^{s_R^*} s^{*b} \frac{1}{2\pi} \log \frac{r}{s^*} ds^* \right\} \\ &= \sum_b \alpha_{j,b}^* \left\{ \frac{1}{2\pi} \left[\frac{s_R^{*b+1}}{b+1} \log s_R^* - \frac{s_R^{*b+1}}{(b+1)^2} \right] \right. \\ &\quad \left. + \frac{u_R - u_i}{2} \sum_{k=0}^{N_g-1} w_k \left(s^{*b} \frac{1}{2\pi} \log \frac{r}{s^*} \frac{ds}{du} \right)_k \right\} \end{aligned} \quad (33)$$

During derivation an identity relation $\log r = \log s^* + \log(r/s^*)$ is used, observing that $r/s^* \rightarrow 1$ as $r \rightarrow 0$. Note that the singular part is integrated analytically and the remaining integral becomes regular, and hence a numerical quadrature can be applied. We may apply the similar expression to the left-hand side of the segment to complete the computation of the self-induced potential due to source. To determine the coefficients $\alpha_{j,b}^*$ in (33), we need to select $p + 1$ or more points on each side of the panel, which may be located on the Gaussian legs, and to form simultaneous equations, which may be solved either by the Gaussian reduction or by the least square approach.

5.2 Self-Induced Potential due to a Rankine Dipole

The induced potential due to a Rankine dipole of constant strength can be expressed by the subtended angle term and the remaining Cauchy integral as follows:

$$\begin{aligned} I_{0,self}^D &= \frac{1}{2\pi} \int \hat{n} \cdot \nabla \log r ds \\ &= \frac{1}{2\pi} \int \hat{n} \cdot \frac{-\vec{r}}{r^2} ds \\ &= -\frac{1}{2} + \frac{1}{2\pi} \int \hat{n} \cdot \frac{-\vec{r}}{r^2} ds \end{aligned} \quad (34)$$

where the distance vector \vec{r} is defined by a vector extending from the source point on the panel surface to the control point. Note that the Cauchy integral is regular and causes no numerical integration problem as long as the zero point is avoided. By separating the integration range into two regions at the control point as in the source integral, each region may employ a proper Gaussian quadrature avoiding the singular point appearing at the integration boundary.

Since the higher order terms are less singular than the constant strength term, the same numerical procedure may be applied to achieve the same degree of accuracy.

5.3 Induction due to Non-Singular Integrands

Evaluation of the potential induced by non-singular integrands will not cause any problem. Being regular, the integration can be performed by employing a proper numerical quadrature. This may occur for the self-induction due to regular parts in (30) or for the far-field control point which is located away from the singular panel. Since the procedure is identical, we will show only the numerical formulation for the far-field potential. The far-field potential due to a dipole panel whose strength is represented by (28) may be expressed as:

$$\begin{aligned} I_{far}^D &= \sum_n \int_n \phi \frac{\partial G}{\partial n} ds \\ &= \sum_n \int_n \sum_j \phi_j^v N_j(u) \frac{\partial G}{\partial n} \frac{ds}{du} du \\ &= \sum_n \sum_j \phi_j^v \int_n N_j(u) \frac{\partial G}{\partial n} \frac{ds}{du} du \\ &\simeq \sum_n \sum_j \phi_j^v \left\{ \frac{u_R - u_L}{2} \sum_k w_k \left(N_j(u) \frac{\partial G}{\partial n} \frac{ds}{du} \right)_k \right\} \end{aligned} \quad (35)$$

Since the control point is away from the dipole, to evaluate (35), we may use the Gaussian quadrature, which is valid when the field point is sufficiently far from the dipole panel. Existing numerical quadrature with selection of the proper order, say order ≤ 4 , can be used. The criterion, Cr , for the measure of the far distance may be defined by the ratio of the distance from the centroid of the panel to the field point, d , and the characteristic length of the panel, ℓ , as $Cr = d/\ell$.

When the field point is not sufficiently far from the singularity panel, the integrand will vary rapidly, thus requiring higher order of numerical quadrature. When the control point is considered too close to the panel, the panel may be subdivided into 2 or more subpanels and the induction integrals may be evaluated with the subpanels. This subdivision process may be repeated until the predetermined criterion is satisfied.

6 Solution of Linear Systems

The number of unknown potential vertices N^v is greater than the number of the panels since $N^v = N^\phi + p$. Hence, if the domain of integration coincides with the range of the integral equation, we have to place more than one control points on each panel in order to prevent the resulting linear system to be underdetermined. However, since the equation (25) is overdetermined, we can place one control point on each panel in S and N^W ($N^W \geq p$) control points on W .

If $N^W = p$, the resulting linear system becomes square. Applying the relations (31) through (35), into the integral equation (30) for N^v control points, we will obtain a square linear system(denoted **ovGrSqHi** in Tables and Figures) for N^v potential vertices as follows:

$$\mathbf{A}\phi^v = \mathbf{B} \tag{36}$$

where \mathbf{A} is $N^v \times N^v$ matrix, ϕ^v the unknown potential vertex strength vector and \mathbf{B} the forcing vector with N^v elements. This system can easily be solved by Gauss elimination.

The number of control points on W is closely related with the mode number of irregular frequencies. For example, p control points on W are sufficient for the system, **ovGrLo**, (24), to have a unique solution as long as the wavenumber is smaller than the $(p + 1)$ th irregular frequency of the original Green integral equation (22) when the wetted surface possesses symmetry with respect to the y axis. If we need solutions of (36) for high frequency range, we have to employ B-spline functions of very high degree. In principle, we can employ B-spline functions of any degree but, in practice, the fourth degree B-spline basis functions are sufficient since they provide the continuities of the potential and its derivatives to the third order along the wetted surface of the body. In this case, say $p = 4$, the uniqueness of the solution of the square system (36) is guaranteed only for the wavenumber smaller than the fifth irregular frequency.

If we want to have solutions for high frequency range while fixing the degree p to 4, it can be done by introducing a redundant linear system(denoted **ovGrRechI** in Tables and Figures) which can be constructed by placing sufficient number N^W ($N^W > 4$) of control points on W as follows:

$$\mathbf{A}_r\phi^v = \mathbf{B} \tag{37}$$

where \mathbf{A}_r is $N^{CP} \times N^v$ matrix with $N^{CP} = N^\phi + N^W$. This system can be solved by a least square approach.

Table 1. Hydrodynamic coefficients calculated at irregular frequencies by low order panel methods applying (16) and (24) respectively for the improved and overdetermined Green integral formulation.

$k_o D$	Linear system	Sway		Heave	
		m_{11}	b_{11}	m_{22}	b_{22}
3.636	imGrLo	0.196046	0.818564	0.705396	0.281423
	ovGrLo	0.196225	0.817878	0.705132	0.281481
6.504	imGrLo	0.201513	0.517204	0.828620	0.095391
	ovGrLo	0.201216	0.517340	0.828554	0.095426
9.56	imGrLo	0.240776	0.343718	0.888871	0.037996
	ovGrLo	0.240922	0.343254	0.888777	0.037863

We have also constructed a redundant linear system(denoted **GrRecHi** in Tables and Figures) which shows the influence of irregular frequencies in (22) as follows:

$$\mathbf{A}_s \phi^v = \mathbf{B} \quad (38)$$

where \mathbf{A}_s is $N^{CP} \times N^v$ matrix with $N^{CP} = 2 \times N^\phi$ and all the control points are on the wetted surface S .

7 Numerical Results and Discussions

A half immersed circular cylinder, of the diameter $D = 1$, oscillating on the free surface of deep water as shown in Figure 1 is selected for numerical tests.

7.1 Validation of Overdetermined Green Integral Formulation

The first task is to show, in the framework of the low order panel method, that the overdetermined Green integral equation (25) gives correct numerical results in predicting the hydrodynamic coefficients through the direct comparison with those of the improved Green integral equation (13) which has already been proved in Hong[Hong, 1987]. Table 1 shows the hydrodynamic coefficients at the first three irregular frequencies of the original Green integral equation (22), calculated using both the equations of the low order square linear system, **imGrLo**, (16) and the low order overdetermined linear system, **ovGrLo**, (24). The wavenumbers are nondimensionalized by the diameter of the circular cylinder as $k_o D$. The number of low order panels used in (16) is $N = 50$ on the wetted surface S and $M - N = 6$ on the inner free surface W . The same number of panels is used for (24) on S together with 6 control points on W . The differences are shown to be of order 10^{-4} , and are almost negligible considering single precision computation.

The next step is to show that the overdetermined Green integral, which is just proved valid for the low order panel method, can be applied to the higher order panel method. The hydrodynamic coefficients at the same irregular frequencies as in Table 1 are calculated using the equations of the higher order square system, **ovGrSqHi**, (36) and of the higher order redundant system,

Table 2. Hydrodynamic coefficients calculated at irregular frequencies by higher order panel methods applying (36) and (37) respectively for square and redundant systems of equations based upon overdetermined Green integral formulation.

$k_o D$	Linear system	Sway		Heave	
		m_{11}	b_{11}	m_{22}	b_{22}
3.636	ovGrSqHi	0.195881	0.817760	0.705391	0.280472
	ovGrRecHi	0.195883	0.817758	0.705394	0.280473
6.504	ovGrSqHi	0.201054	0.515586	0.828781	0.094790
	ovGrRecHi	0.201055	0.515585	0.828790	0.094766
9.56	ovGrSqHi	0.240910	0.341721	0.889036	0.037292
	ovGrRecHi	0.240923	0.341706	0.889096	0.037159

ovGrRecHi, (37), and compared in Table 2. The number of higher order panels used by (36) is $N^\phi = 10$ on the wetted surface, on each of which one control point is placed together with five control points ($N^W = 5$) on the inner free surface W . The degree of B-spline basis functions is $p = 5$. The same number of higher order panels with one control point per panel are used by (37) on S but $N^W = 6$ on W , and at the same time the degree of B-spline basis functions is lowered to $p = 4$. The differences are shown to be of order 10^{-5} which are indistinguishable under single precision computation. From Tables 1 and 2, we may now conclude that the overdetermined Green integral formulation predicts the hydrodynamic coefficients even at the irregular frequencies.

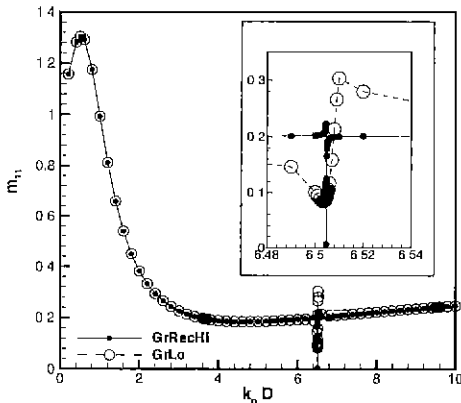


Figure 2. Irregular frequencies in sway added mass coefficients computed by **GrLo** (21) and **GrRecHi** (38), based on original Green integral formulation.

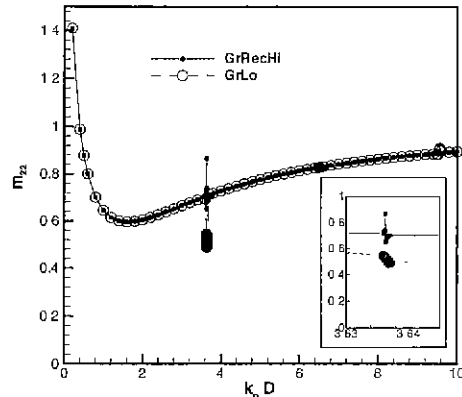


Figure 3. Irregular frequencies in heave added mass coefficients computed by **GrLo** (21) and **GrRecHi** (38), based on original Green integral formulation.

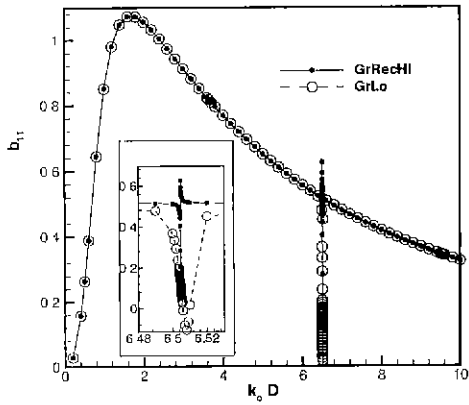


Figure 4. Irregular frequencies in sway wave damping coefficients computed by **GrLo** (21) and **GrRecHi** (38), based on original Green integral formulation.

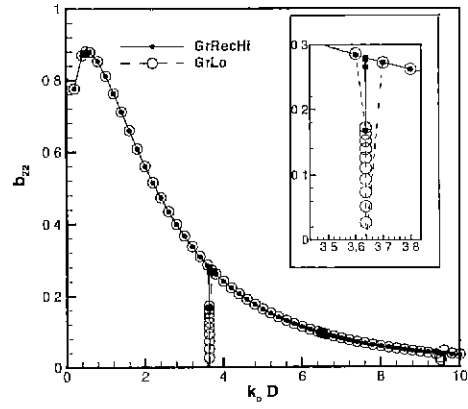


Figure 5. Irregular frequencies in heave wave damping coefficients computed by **GrLo** (21) and **GrRecHi** (38), based on original Green integral formulation.

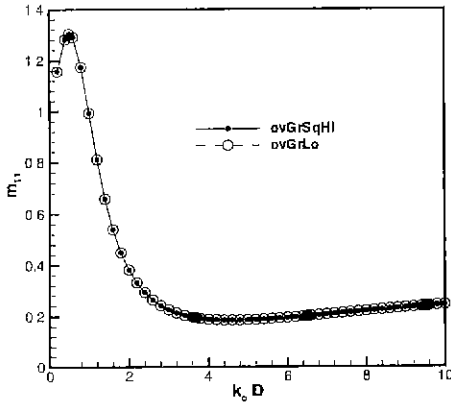


Figure 6. Sway added mass coefficients computed by **ovGrLo** (24) and **ovGrSgHi** (36) based on overdetermined Green integral formulation.

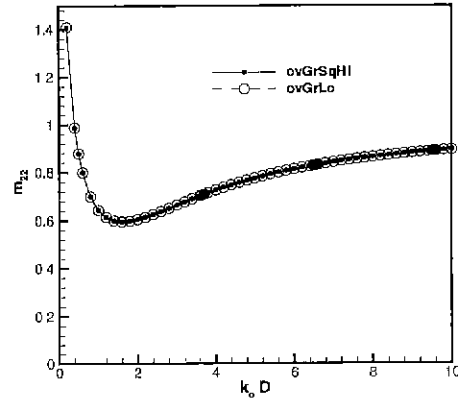


Figure 7. Heave added mass coefficients computed by **ovGrLo** (24) and **ovGrSgHi** (36) based on overdetermined Green integral formulation.

7.2 Performance of Higher Order Panel Method

We now demonstrate the performance of the higher order panel method based on B-splines, mostly with figures to show the general behavior of the computed results. We first show that the irregular frequency still exists in the higher order method if formulated based on the original Green integral equation, as shown in Figures 2 ~ 5. The number of low order panels used by the system, **GrLo**, (21) is $N = 50$ on S . The number of higher order panels used by the system, **GrRecHi**, (38)

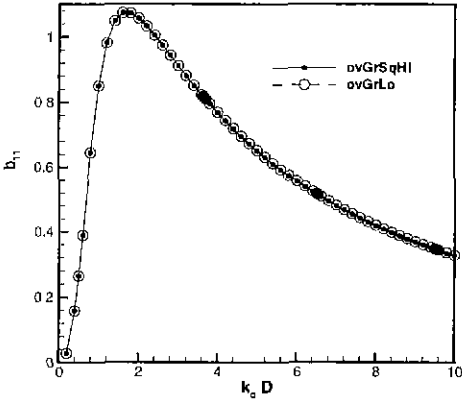


Figure 8. Sway wave damping coefficients computed by **ovGrLo** (24) and **ov-GrSqHi** (36) based on overdetermined Green integral formulation.

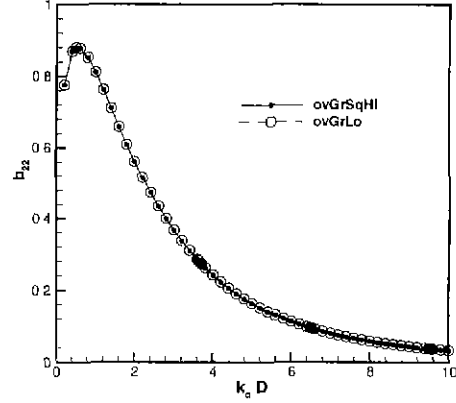


Figure 9. Heave wave damping coefficients computed by **ovGrLo** (24) and **ov-GrSqHi** (36) based on overdetermined Green integral formulation.

is $N^\phi = 20$ on S with two control points placed per panel. Figures clearly show the existence of the irregular frequencies, whose positions are dependent upon the mode of oscillations. The detailed behavior around the irregular frequencies are magnified on each figure, which shows that the deteriorated wave number band of the higher order method is much narrower than that of the low order method. In the present computation, the wavenumbers are varied by $\Delta(k_0 D) = 0.0001$ in the neighborhood of the already-known irregular frequencies.

Finally, the hydrodynamic coefficients computed by the B-spline higher order panel method using the system, **ovGrSqHi**, (36) are compared with those computed by the low order panel method using the system, **ovGrLo**, (24) as shown in Figures 6 ~ 9. The number of higher order panels is $N^\phi = 10$ on the wetted surface S and one control point are used per panel together with five control points ($N^W = 5$) on the inner free surface W . And the degree of B-spline basis functions is $p = 5$. The number of low order panels is $N = 50$ on S and 6 control points is used on W . As expected, the irregular frequencies are completely removed, leading to the conclusion that the higher order technique can be a good alternative to the already-proved low order panel method in computing the behavior of the floating bodies on the free surface. The ability of B-splines that guarantees higher order derivatives of the basis functions may become a deciding factor in selecting the proper method between the low and higher order formulations.

8 Conclusions

An overdetermined Green integral equation applied to the radiation wave problem for a two-dimensional body oscillating on the free surface has been presented. Its solution has been shown to be identical with that of the improved Green integral equation.

A square linear system as well as a redundant linear system according to the B-spline higher order panel method have been constructed from the overdetermined Green integral equation. Nu-

merical tests show that the two systems are equivalent in precision but the former is more economic in computation, since the size of the matrix of the former is far smaller than that of the latter.

Since the B-splines have analytical derivatives of any order, the present method can better be applied to the problem requiring higher order derivatives, for example, to the second order potential problem of time-varying drift force calculation.

References

1. Hess, J.L. and Smith, A.M.O., 1964, Calculation of Nonlifting Potential Flow About Arbitrary Three-Dimensional Bodies, *Journal of Ship Research*, **8**, **2**
2. Hong, D.-C., 1984, Discrétisation du contour d'une tranche de navire en vue de la résolution numérique du problème de radiation-diffraction, Rapport No. 8422, Laboratoire d'Hydrodynamique Navale, ENSM de Nantes, France
3. Guevel, P., Kobus, J.M., 1975, Flotteurs cylindriques horizontaux soumis à des oscillations forcées de très faible amplitude, *Bulletin de l'ATMA*, **75**, Paris
4. Hong, D.-C., 1987, On the Improved Green Integral Equation Applied to the Water-Wave Radiation-Diffraction Problem. *Journal of SNA of Korea*, **24**, **1**
5. Kobus, J.M., 1976, Application de la méthode des singularités aux problème des flotteurs cylindriques soumis à des oscillations harmoniques forcées de faible amplitude, Thèse de Docteur-Ingénieur, Laboratoire d'Hydrodynamique Navale, ENSM de Nantes, France
6. Ohmatsu, S., 1983, A New Simple Method to Eliminate the Irregular Frequencies in the Theory of Water Wave Radiation Problem, *Papers of the Ship Research Institute No.70*, Japan
7. Kleinman, R.E., October 1982, On the mathematical theory of motion of floating bodies-An update, Report DTNSRDC-82/074
8. John, F., 1950, On the Motion of Floating Bodies II., *Communications on Pure and Applied Mathematics*, **3**.
9. Lee, C.-S., Kerwin, J.E., 1999, *A B-Spline Higher-Order Panel Method Applied to Two-Dimensional Lifting Problem*. Submitted for publication